

Flavin-Mediated Photoactivation Of Pt(IV) Anticancer Complexes: Computational Insights On The Catalytic Mechanism

Stefano Scoditti,^a Eslam Dabbish,^a German E. Pieslinger,^b Elixabete Rezabal,^{c,d} Xabier Lopez,^{c,d}
Emilia Sicilia,*^a Luca Salassa*^{c,d,e}

^a Department of Chemistry and Chemical Technologies, Università della Calabria, Arcavacata di Rende (CS), 87036, Italy

^b CONICET – Universidad de Buenos Aires, Instituto de Química y Fisicoquímica Biológicas (IQUIFIB), Buenos Aires, Argentina

^c Donostia International Physics Center, Paseo Manuel de Lardizabal 4, Donostia, 20018, Spain

^d Polimero eta Material Aurreratuak: Fisika, Kimika eta Teknologia, Kimika Fakultatea, Euskal Herriko Unibertsitatea UPV/EHU, Paseo Manuel de Lardizabal 3, Donostia, 20018, Spain

^e Ikerbasque, Basque Foundation for Science, Bilbao, 48011, Spain

Electronic Supplementary Material (ESI)

Table S1 Imaginary frequencies for all computed transition states.

NADH:Rf → NAD ⁺ :RfH ⁻	
¹ TS	-1544.79
³ TS	-506.97
RfH ⁻ :Pt(IV) → Rf:Pt(II) – Complex 1	
TS (Pt–O1 attack)	-111.31
TS (acetyl O2 attack)	-592.10
RfH ⁻ :Pt(IV) → Rf:Pt(II) – Complex 2	
TS (Pt–O1 attack)	-113.23
TS (acetyl O2 attack)	-113.15
NADH:Pt(IV) → NAD ⁺ :Pt(II) – Complex 1	
TS (Pt–O1 attack)	-1265.22
TS (acetyl O2 attack)	-1194.61
NADH:Pt(IV) → NAD ⁺ :Pt(II) – Complex 2	
TS (Pt–O1 attack)	-1352.04
TS (acetyl O2 attack)	-1139.99
AscH ⁻ :Pt(IV) → DHAsc [‡] :Pt(II) – Complex 1	
TS (Pt–O1 attack)	-1141.66
TS (acetyl O2 attack)	-189.16
AscH ⁻ :Pt(IV) → DHAsc [‡] :Pt(II) – Complex 2	
TS (Pt–O1 attack)	-655.29
TS (acetyl O2 attack)	-194.17

[‡] DHAsc = Dehydroascorbate

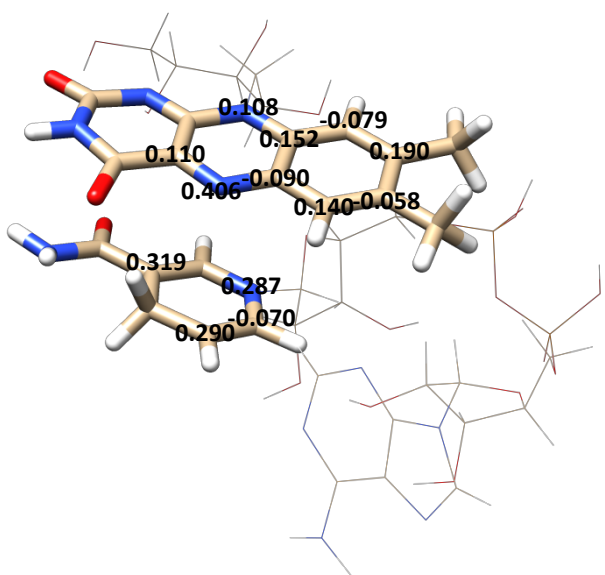


Fig. S1 Mulliken spin density of the initial adduct ${}^3[\text{NADH}:\text{Rf}]$ for atoms having values > 0.100 or < -0.050 .

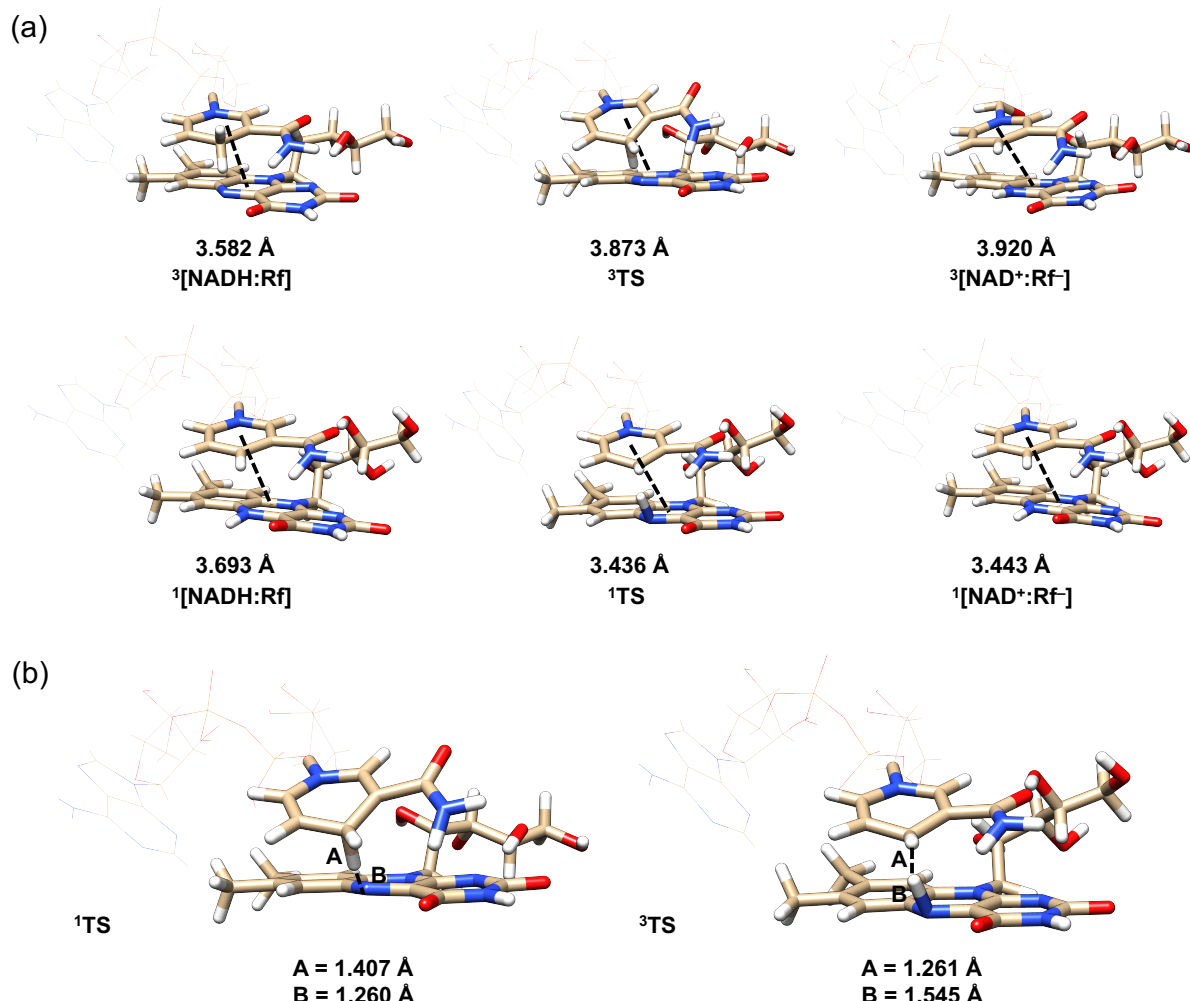


Fig. S2 Calculated models for the reaction between NADH and Rf in both singlet ground and triplet excited-states. Distances between the stacked adducts are shown in (a), while (b) reports the $\text{C}(6)_{\text{NAD}}-\text{H}-\text{N}(5)_{\text{Rf}}$ bond lengths.

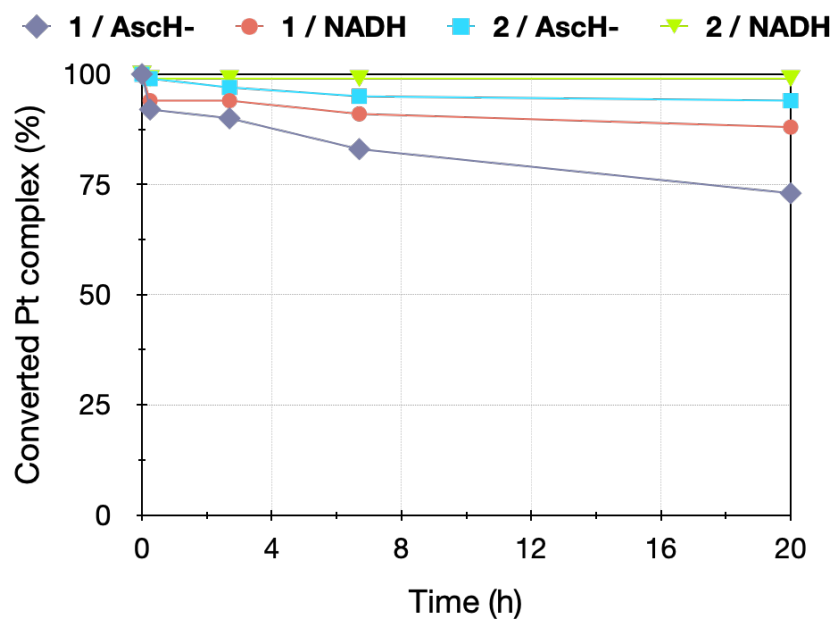


Fig. S3 Experimental reduction rates of **1** and **2** for AscH^- and NADH over 20 h in the dark. Reactions were performed in PB buffer (10 mM, pH 7.4) using 1 mM of reducing agent. Under similar experimental conditions, light-generated RfH^- (catalytic, 5% catalyst load) achieves full conversion of the two complexes in less than 4 min.¹

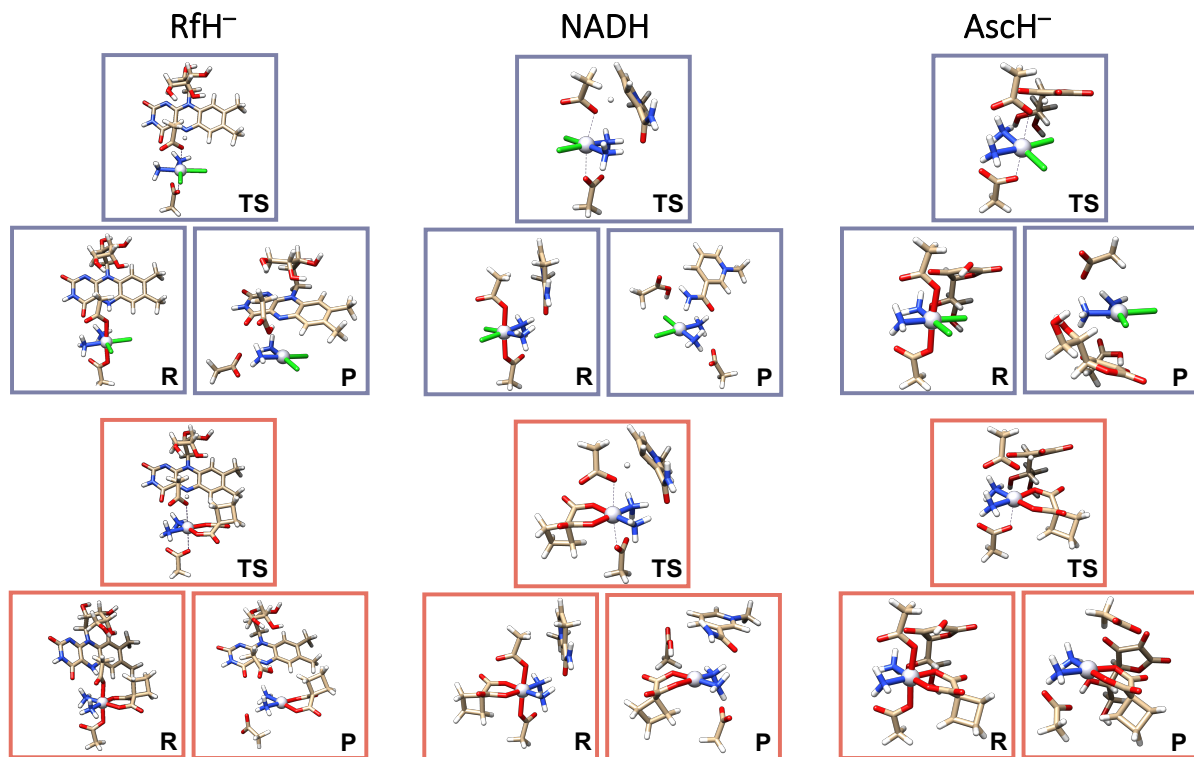


Fig. S4 Models of initial adduct (R), transition state (TS) and product (P) for the reduction of complexes **1** (violet) and **2** (red) by RfH^- , NADH and Asch^- . Optimized geometries were obtained assuming that the Pt-coordinated O(1) atom of an axial acetato ligands of **1** and **2** interacts with the hydride donating moiety of the donor.

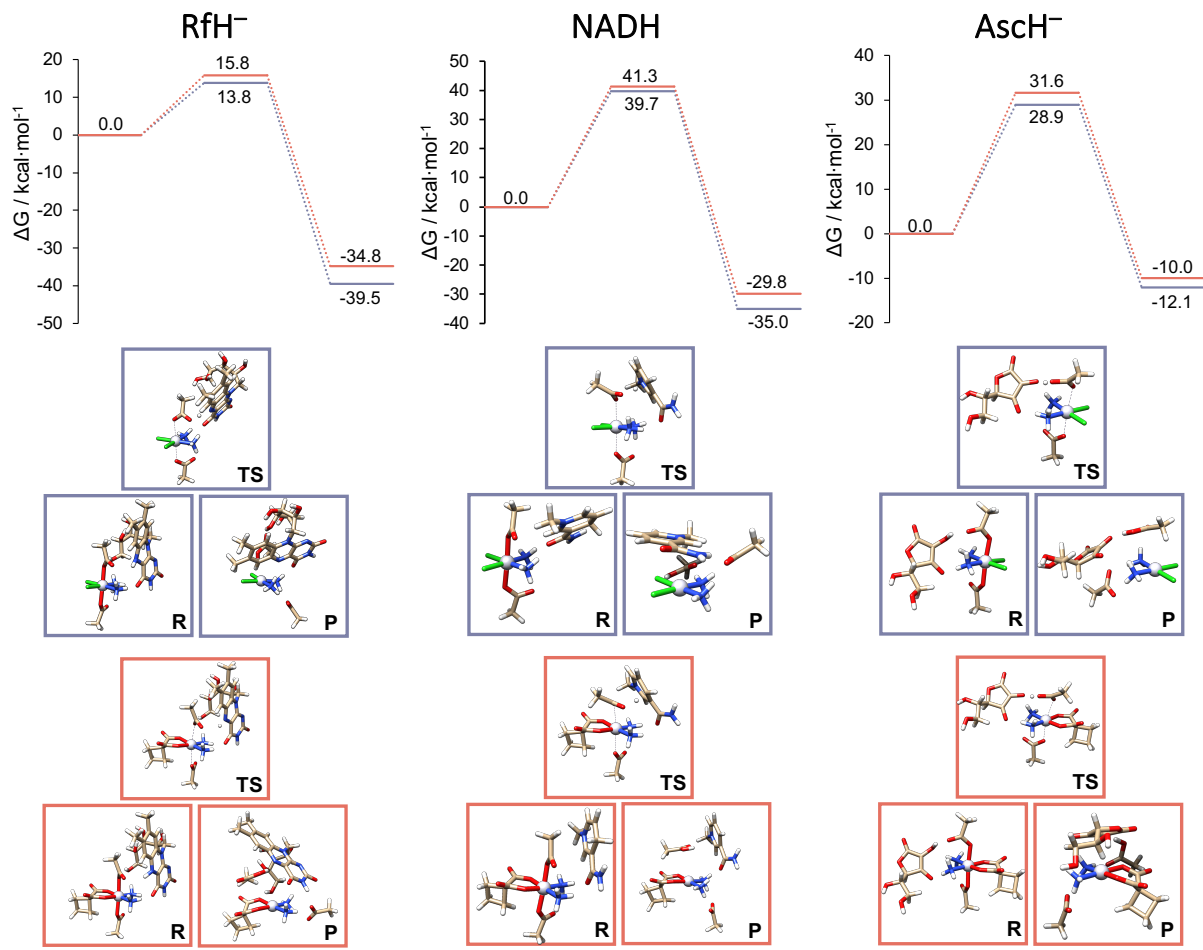


Fig. S5 Free energy profiles describing the ligand-bridged-H-transfer mechanism for the reduction of complexes **1** (violet) and **2** (red) by RfH⁻, NADH and Asch⁻. Models of initial adduct (R), transition state (TS) and product (P) were obtained assuming that the carbonyl O(2) atom of an axial acetato ligands of **1** and **2** interacts with the hydride donating moiety of the donor. Relative energies are expressed in kcal mol⁻¹ and calculated with respect to the zero-reference energy of the initial adduct (in the singlet ground state).

References

- 1 J. Gurruchaga-Pereda, V. Martínez-Martínez, E. Rezabal, X. Lopez, C. Garino, F. Mancin, A. L. Cortajarena and L. Salassa, *ACS Catal.*, 2020, **10**, 187–196.